A novel NOLM structure with nonreciprocal phase shift bias for power fluctuation reduction of pulse trains

Liwei Guo (郭力为), Xue Feng (冯 雪), Yue Liu (刘 越), and Xiaoming Liu (刘小明)

Department of Electronic Engineering, Tsinghua University, Beijing 100084

Received May 9, 2006

A novel nonlinear optical loop mirror (NOLM) with a nonreciprocal phase shift bias (NPSB), called power equalization NOLM (PE-NOLM), is proposed for reducing the power fluctuation of pulse trains. NPSB provides part of the nonreciprocal phase difference so that the required input power is reduced, and nonsymmetrical coupling ratio of coupler can adjust the transmission curve to improve the equalization range. It has been shown theoretically that compared with earlier PE-NOLM, about 1.6 dB of equalization power reduction and about 2.2 dB of equalization range enhancement could be achieved. Experiments have demonstrated that the output power fluctuation is reduced to less than 0.4 dB, while the required input peak power range is 4.5 dBm (15.6—20.1 dBm).

OCIS codes: 060.0060, 190.4370.

Ultrahigh-speed optical pulse trains have wide applications in optical communication systems. However, for most common laser sources, enhancement of the repetition rate would generally increase amplitude fluctuations in a noise form due to slow gain dynamics in harmonically mode-locked lasers[1], or in a periodic form when repetition-rate multiplication techniques such as subharmonic optical injection[2] are used. Therefore, reduction of amplitude fluctuations, or power equalization, is an important issue in making the high-speed optical pulse trains applicable. Different techniques[3−8] have been studied for reducing power fluctuations. Among them, nonlinear optical loop mirror (NOLM) is particularly attractive for its capability of reducing random or deterministic power fluctuations with a very short response time (∼fs) of Kerr effect, without requiring additional pump signal. The reflection and transmission function of a NOLM is sinusoidal and power-dependent. Therefore, if the input power of the pulse trains fluctuates around the point that brings maximum output power, the output power fluctuation would be limited, which is the principle of power equalization NOLM (PE-NOLM).

The earliest PE-NOLM was proposed in Ref. [8], where a power-symmetric coupler was used to construct the loop and the reflection port was used as the output. The amplitude fluctuation was reduced from 2.2 to 0.46 dB for a 38-GHz pulse train. Generally, the reflection port was employed as the output in NOLM application, because the required phase difference between clockwise (CW) and counter-clock-wise (CCW) lightwaves to achieve the first maximum is about $\pi/2$ and π for the reflection port and the transmission port respectively, where the required input power would be much lower for the former case. In fact, the required input power is rather high, even if the reflection port is used. In addition, another drawback of the earliest PE-NOLM is that, the shape of the reflection curve is fixed so that the output power may drop to form a notch due to destructive interference as input power increases. This would limit the equalization range (ER), which is the maximum input power range corresponding to a given output fluctuation.

A PE-NOLM with adjustable transmission curve was proposed in Ref. [9], where 500-m highly twisted standard single-mode fiber (SMF-28) and a quarter-wave plate (QWP) were inserted asymmetrically to introduce polarization asymmetry. By rotating the QWP, the shape of the transmission curve can be changed so that the ER may be enhanced. However, this is achieved at the expense of increasing input power.

In this paper, a novel PE-NOLM that can simultaneously achieve large ER as well as low input power by adjusting the transmission characteristics is obtained by introducing a nonreciprocal phase shift bias (NPSB) and a power-asymmetric coupler in the loop, where the transmission port is used for output. The NPSB device can provide a power-independent linear phase difference between CW and CCW lightwaves, which can dramatically reduce the required nonlinear phase difference, i.e. the required input power. As a result, the transmission port can be employed in the PE-NOLM without the need for high input power. More importantly, this novel PE-NOLM can remove the unwanted notch on the transmission curve by properly selecting the ratio of the coupler.

The schematic setup of the proposed PE-NOLM is shown in Fig. 1, where the power coupling ratio is $\alpha : (1-\alpha)$. So the input power of $P_{\rm in}$ is split unequally. An attenuator/amplifier with a loss/gain of G is set near one of the coupler's ports to achieve power asymmetry, while a NPSB device is placed to provide phase bias. NPSB can be realized by various methods[10,11]. The output power

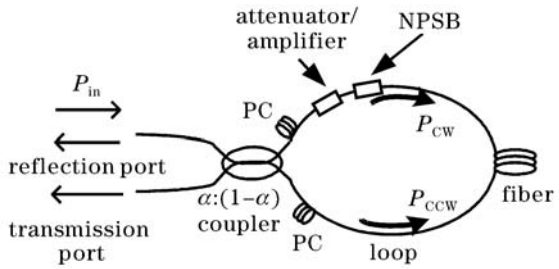

Fig. 1. Schematic structure of the proposed PE-NOLM.

at the reflection port and the transmission port, $P_{\rm R}$ and $P_{\rm T}$ can be written as[12]

$$P_{\rm R} = 2G\alpha\,(1-\alpha)\,P_{\rm in}\cdot\left[1+\cos\left(\pi\frac{P_{\rm in}}{P_\pi}+\varphi_{\rm bias}\right)\right], \quad (1)$$

$$P_{\rm T} = [1-2\alpha\,(1-\alpha)]\,GP_{\rm in} \cdot\left[1-\frac{2\alpha\,(1-\alpha)}{1-2\alpha\,(1-\alpha)}\cos\left(\pi\frac{P_{\rm in}}{P_\pi}+\varphi_{\rm bias}\right)\right], \quad (2)$$

where $P_\pi = \pi/\{[1-(1+G)\,\alpha]\,\gamma L_{\rm eff}\}$ is the special input power that makes the nonlinear phase difference between the CW and CCW lightwaves as π, γ and $L_{\rm eff}$ are the nonlinear coefficient and the effective length of the loop's fiber, respectively. $P_{\rm in}/P_\pi$ can be considered as the normalized input power, which is determined by the nonlinear effect along the loop, regardless of G, γ and $L_{\rm eff}$. $\varphi_{\rm bias}$ is the value of NPSB, which is dependent on the device but independent of the optical power. There is a term of $M = \frac{2\alpha(1-\alpha)}{1-2\alpha(1-\alpha)}$ in the front of the cosine function in Eq. (2), which reflects the interference at the transmission port and is determined by the coupling ratio α. By changing the value of α, M can be less than 1 and the deep notch at the transmission curve can be adjusted or even eliminated. But in Eq. (1), the coefficient of cosine is constantly 1, so the coupling ratio affects only the total reflected power but not the shape of the reflection curve.

Figure 2 shows the curves of output power versus normalized input power calculated by Eqs. (1) and (2), respectively. The solid line is the reflected curve with $\varphi_{\rm bias} = 0$ and $\alpha = 0.5$, where the output power drops to zero when $P_{\rm in}/P_\pi = 1$, due to perfect destructive interference. The dashed line and dotted line are the transmission curves with $\varphi_{\rm bias} = 1.5\pi$, $\alpha = 0.5$ and $\alpha = 0.32$, respectively. Comparing to the solid line, the input power corresponding to the output maximum peak is much lower for the dashed line due to the contribution of NPSB; while the notch is almost eliminated with a properly chosen α (the dotted line).

By taking no more than 0.4 dB output fluctuation as the criterion, we can find out the corresponding input power range (i.e. ER) from the transmission curves. Figure 3(a) shows the contour map of transmitted ER versus the coupling ratio α and NPSB $\varphi_{\rm bias}$, where the darker

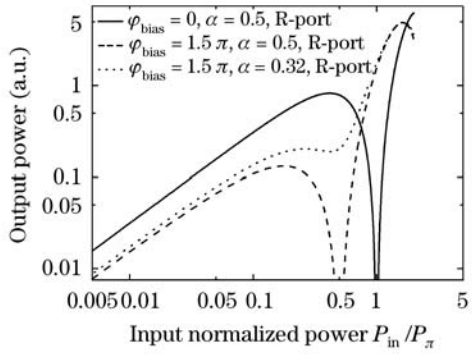

Fig. 2. Output power of PE-NOLM versus normalized input power for several values of α and $\varphi_{\rm bias}$.

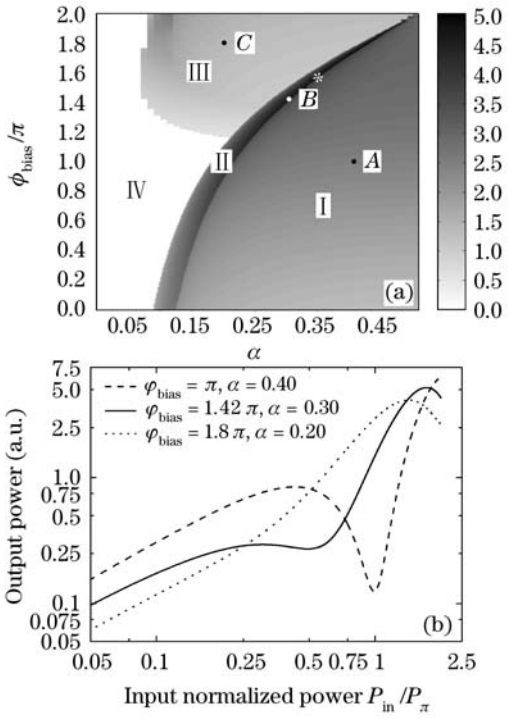

Fig. 3. Calculated results for PE-NOLM. (a) Altitudinal map of ER versus α and $\varphi_{\rm bias}$; (b) transmitted power versus normalized input power for several values of α and $\varphi_{\rm bias}$.

the color, the larger the resulted ER. It can be seen that, the map is divided into four areas, the largest ER lies in a narrow belt of area II. Figure 3(b) shows three typical transmission curves. The dashed line, being a typical curve in area I, has the coordination of $\varphi_{\rm bias} = \pi$, $\alpha = 0.40$ (point A). By using the maximum peak at $P_{\rm in}/P_\pi \approx 0.4$, ER is about 2.5 dB. Within area I, NPSB is rather small or the coupling ratio is close to 0.5, so the curve is more cosine-like and the notch is clear. The solid line corresponds to $\varphi_{\rm bias} = 1.42\pi$ and $\alpha = 0.30$ (point B in area II), where the notch is almost eliminated, ER is increased to about 4.5 dB. For the dotted line ($\varphi_{\rm bias} = 1.8\pi$, $\alpha = 0.20$, point C in area III), the notch is over-raised so that one may miss the first maximum peak. In this case, the second peak is located in the range of $1 < P_{\rm in}/P_\pi < 2$, and ER is quite narrow. For area IV (the corresponding curve is not shown in Fig. 3(b)), the output power increases monotonously with the input power until $P_{\rm in}/P_\pi \le 2$; the second maximum peak may require even higher input power, which is beyond our scope.

Figures 4(a) and (b) are the contour maps of equalization power (EP) and transmission ratio (TR) versus α and $\varphi_{\rm bias}$, respectively. Here, EP is defined as the average input power over the equalization range, while TR is defined as

$$\mathrm{TR} = \frac{P_{\rm T}}{P_{\rm T}+P_{\rm R}}, \quad (3)$$

when the input is the mean power over the equalization range, representing the efficiency of PE-NOLM. Like ER map, both EP and TR maps are divided into four areas. Area IV, filled with black and white, has no physical meaning, because no equalization range has been found

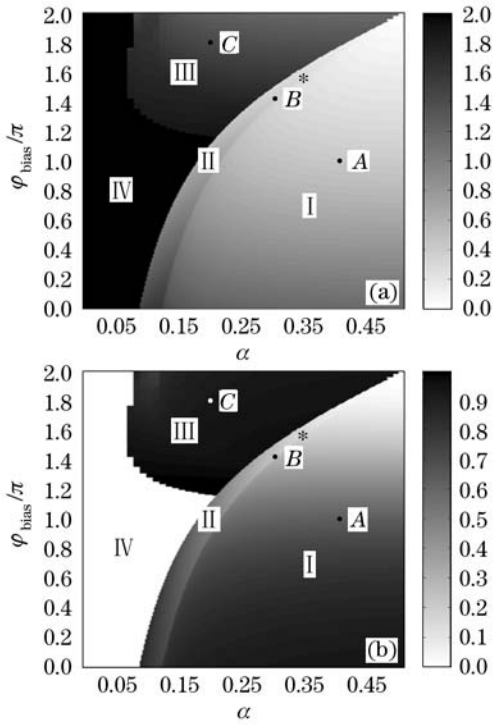

Fig. 4. Calculated altitudinal maps for PE-NOLM. (a) EP versus α and $\varphi_{\rm bias}$; (b) TR versus α and $\varphi_{\rm bias}$.

in this area. For areas I and II, it can be seen that increasing NPSB would bring a reduction in EP but a lower TR as well. This is easy to be understood that, destructive interference is used to lower the high power pulse as equal as the low power ones, thus loss mechanism is introduced intrinsically. NPSB replaces part of the input power to create phase difference, so the input power is reduced but the loss is still there. The more NPSB introduced, the more serious the destructive interference effect is, and therefore, there would be more loss penalty. Fortunately, the loss can be compensated easily by a following gain-equalized erbium-doped fiber amplifier (EDFA).

As a summary, parameters α and $\varphi_{\rm bias}$ must be properly chosen considering the trade-off among ER, EP and TR. For example, we can choose $\alpha = 0.343$ and $\varphi_{\rm bias} = 1.57\pi$ (the asterisk in Fig. 3(a)). From the calculated data, the required input power is $0.15P_\pi - 0.44P_\pi$, the achieved results are ER = 4.7 dB and EP = $0.29P_\pi$ with a loss of 8.4 dB. For comparison, similar calculation is carried out for a previous PE-NOLM with $\varphi_{\rm bias} = 0$, $\alpha = 0.5$, where the reflection port is used for output. The required input power is $0.30P_\pi - 0.53P_\pi$, ER and EP are 2.5 dB and $0.42P_\pi$ respectively, and the loss is 2.0 dB. So ER is extended by 2.2 dB and EP is reduced by 1.6 dB using our PE-NOLM, while 6.4 dB loss is added.

An experiment to validate the proposed novel PE-NOLM was preformed using the setup in Fig. 5. In Fig. 5(a), the loop consists of a 0.343:0.657 coupler, 10-km dispersion-compensated fiber (DCF), two polarization controllers (PC2 and PC3) and two acousto-optic modulators (AOMs). The AOMs with a piece of single mode fiber (SMF) in between act as the NPSB device, where $\rm AOM^+$ and $\rm AOM^-$ are NEOS N26027 1st and NEOS N26027 −1st, providing frequency shift of +27 and −27

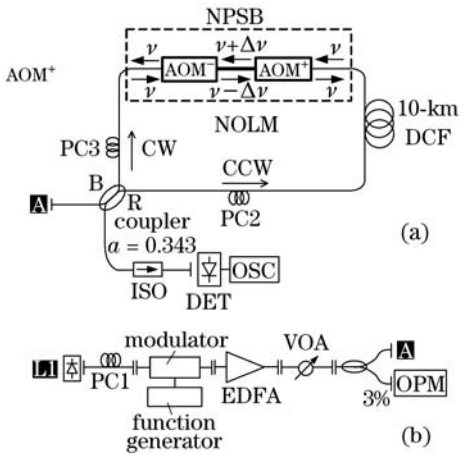

Fig. 5. Experimental setup. (a) Detail configuration of PE-NOLM; (b) input signal generation setup.

MHz respectively, when the modulation signal is not applied. The length of SMF between the AOMs is 660 cm. The frequency of CW lightwave is down-shifted firstly by $\rm AOM^+$ and shifted back by $\rm AOM^-$, while that of CCW lightwave is shifted in a reverse order. So the two lightwaves have different frequencies, therefore there is a phase difference between them when they propagate along the 660-cm fiber. The resulted $\varphi_{\rm bias}$ is 1.57π, calculated by

$$\varphi_{\rm bias} = \frac{4\pi n}{c} l\Delta\nu, \tag{4}$$

where c, n, l and $\Delta\nu$ are the velocity of light in vacuum, refractive index of the fiber, fiber length between the AOMs and shifted frequency in AOM, respectively. The total loss of the two AOMs is about 8 dB, serving as the asymmetrical loss in the PE-NOLM[8]. The nonlinear coefficient, attenuation and dispersion of DCF at 1554 nm are 4 $\rm W^{-1}\cdot km^{-1}$, 0.7 dB/km and −80 ps/(nm·km), respectively. By adjusting the PCs, the influence of residual birefringence on the loop can be compensated[13].

In Fig. 5(b), the optical pulse train with a central wavelength of 1554.2 nm is produced by using a semiconductor distributed feedback (DFB) laser L1 and a $LiNbO_3$ modulator. The full width at half-maximum (FWHM) of the optical pulse is 13.5 ns (corresponding to a frequency of 74 MHz), and the repetition rate is 4.58 MHz. In such a low duty cycle, nonlinear interaction between CW and CCW lightwaves is avoidable[8]. The pulse train is injected into an EDFA followed by a variable optical attenuator (VOA), so adjustable peak power with about 23 dBm at maximum is achieved. Before being launched into the NOLM, the power of pulse train is monitored by a 3:97 coupler and an optical power meter (OPM). A high-speed lightwave converter (DET, Agilent 83440B) and a digital oscilloscope (OSC, Agilent infiniium 54833A) are employed to measure the pulse waveform at the transmission port.

The experimental result of transmitted peak power versus input peak power is shown in Fig. 6, where the circles are the measured data and the solid curve is the calculated result by using the same parameters as in experiment. It can be seen that the experimental results coincide with theoretical ones perfectly. After equalization,

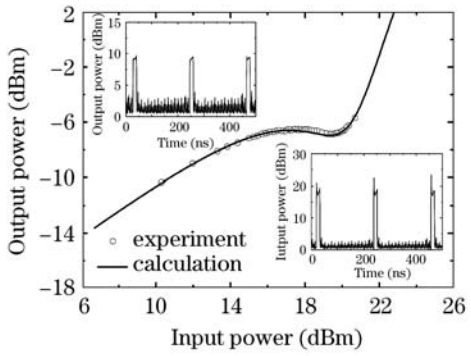

Fig. 6. Experimental transmitted power versus input power compared with a calculated curve, insertions at down-right and up-left are the measured input and output waveforms, respectively.

the 4.5-dB power fluctuation at the input port is reduced to only 0.4 dB, while the required input peak power is only 15.6—20.1 dBm. Insertions in Fig. 6 are the input and output waveforms when the input power is 16.3 dBm. The change in pulse shape is negligible, but the signal-to-noise ratio (SNR) is deteriorated, because the high power pulses experience more interference loss than the noise.

Because of the equipment available, the width of the pulses was limited to 13.5 ns in our experiments. However, the capability of NOLM in ultrahigh-speed ($\sim$ 38 GHz) pulse-train power equalization has already been demonstrated in Ref. [8]. The introduced NPSB utilizes AOM as optical frequency shifter, whose performance is independent of the rate of the pulse train. So it is reasonable to believe that the proposed PE-NOLM would work well for speed up to tens of gigahertz.

In conclusion, we have theoretically and experimentally demonstrated a novel PE-NOLM for reducing the power fluctuation of optical pulse trains, by introducing a NPSB and optimizing the coupling ratio of the NOLM. Theoretically, 1.6-dB equalization power reduction and 2.2-dB equalization range boost have been predicted, compared with previous PE-NOLM. Experiments have shown that the power fluctuation is reduced from 4.5 dB to less than 0.4 dB after equalization, where the required equalization peak power range is 15.6—20.1 dBm.

L. Guo's e-mail address is guoliwei@gmail.com.

References

1. F. Rana, H. L. T. Lee, R. J. Ram, M. E. Grein, L. A. Jiang, E. P. Ippen, and H. A. Haus, J. Opt. Soc. Am. B **19,** 2609 (2002).
2. Y. J. Wen, D. Novak, H. F. Liu, and A. Nirmalathas, Electron. Lett. **37,** 581 (2001).
3. A. Hirano, T. Kataoka, S. Kuwahara, M. Asobe, and Y. Yamabayashi, Electron. Lett. **34,** 1410 (1998).
4. H. J. Lee, K. Kim, and H. G. Kim, Opt. Commun. **160,** 51 (1999).
5. Y. Su, L. Wang, A. Agarwal, and P. Kumar, Electron. Lett. **36,** 1103 (2000).
6. Y. J. Wen, D. Novak, H. F. Liu, and A. Nirmalathas, Electron. Lett. **37,** 581 (2001).
7. K. Yiannopoulos, K. Vyrsokinos, D. Tsiokos, E. Kehayas, N. Pleros, G. Theophilopoulos, T. Houbavlis, G. Guekos, and H. Avramopoulos, IEEE J. Quantum Electron. **40,** 157 (2004).
8. M. Attygalle, A. Nirmalathas, and H. F. Liu, IEEE Photon. Technol. Lett. **14,** 543 (2002).
9. O. Pottiez, E. A. Kuzin, B. Ibarra-Escamilla, F. Gutierrez-Zainos, U. Ruiz-Corona, and J. T. Camas-Anzueto, IEEE Photon. Technol. Lett. **17,** 154 (2005).
10. T. Sakamoto and K. Kikuchi, IEEE Photon. Technol. Lett. **17,** 1058 (2005).
11. I. K. Hwang, S. H. Yun, and B. Y. Kim, Opt. Lett. **22,** 507 (1997).
12. G. P. Agrawal, *Nonlinear Fiber Optics & Applications of Nonlinear Fiber Optics* (in Chinese) D. Jia, Z. Yu, B. Tan, and Z. Hu (translated) (Publishing House of Electronics Industry, Beijing, 2002) pp.355—357.
13. P. Zhang, Y. Liu, and X.-M. Liu, Chin. J. Lasers (in Chinese) **12,** 1645 (2005).